Classical Yang-Mills solutions and iterative maps

Shau-Jin Chang
Department of Physics, University of Illinois at Urbana-Champaign, 1110 W. Green Street, Urbana, Illinois 61801
(Received 26 August 1983)

We study the nonlinear and long-term stability of a constant E field in a Yang-Mills theory by examining the class of solutions discovered by Baseyan *et al.* Using adiabatic invariance, we are able to relate the long-term behavior of the solution to that of an iterative map. We find that the solution is usually chaotic and goes through an endless sequence of seemingly random flips of dominant isospin directions. By a proper choice of initial conditions, we are able to construct two classes of non-self-dual (presumably unstable) periodic solutions. We present the first-few solutions graphically.

I. INTRODUCTION

It is well known that the uniform magnetic field in a classical Yang-Mills field is unstable.[1-3] The unstable modes can lower the energy of the ground state. Ambjørn and Olesen showed that the classical ground state of a Yang-Mills field in the presence of a constant B field is mathematically identical to that of a type-II superconductor.[4] It has been suggested that these magnetic instabilities may be important for understanding color confinement.

A natural question to ask is what is the nonlinear stability of a Yang-Mills electric field. Since we believe that the color confinement is electric in nature, the instability in the electric field may be physically more relevant.

Mandula was the first one to point out that a Yang-Mills Coulomb field may be unstable at large coupling strength.[5] It is easy to see that an infinite-extent uniform electric field cannot be stable under small disturbances. A fluctuation can carry an electric charge. The uniform background electric field can accelerate this charge indefinitely and can deliver an unlimited amount of energy to it. We wish to know whether a nonlinear effect may regulate the energy transfer to the unstable modes. Recently, Jackiw and Rossi[6] showed that a Yang-Mills theory is similar to a gyroscopic system. It is our hope that an analogous gyroscopic force may prevent the unstable solutions from running away.

In this paper, we restrict ourselves to a class of solutions discovered by Baseyan *et al.*[7] In Sec. II we review briefly this class of solutions. It is straightforward to see that a uniform E field is a special case of the above solutions. Thus, we are able to study the stability of a uniform E field within this class of solutions. In particular, we wish to find out how a small disturbance can affect a constant E field in the long run. In Sec. III we use the method of adiabatic invariance to study the time evolution of the solutions. In Sec. VI we are able to relate our trajectory to a simple two-dimensional mapping problem. By making a random-phase approximation, we reduce our iterative problem to a random-walk problem. According to this analysis, we find that the E field changes slowly in one isospin direction but rapidly in other isospin directions. Crossovers from one large isospin direction to another usually take place in a random fashion. This is not unlike the reversals of Earth's magnetic field in a dynamo model.[8] Recently, Nikolaevskii and Shur[9] showed that the above class of solutions is intrinsically nonintegrable and hence proved that a classical Yang-Mills field theory is not exactly solvable. Our result is consistent with their findings.

In addition to the general property of the system, we also study the periodic solutions numerically. By choosing the initial condition properly, we can construct periodic solutions to the Yang-Mills fields. These solutions do not satisfy the self-dual or anti-self-dual condition, and represent a new class of Yang-Mills periodic solutions. In Sec. V we construct and plot the first few periodic solutions numerically. We describe briefly the numerical method in Appendix A.

II. FIELD CONFIGURATIONS

In this paper, we study the time dependence of a class of Yang-Mills solutions. We can extend our solutions to an arbitrary non-Abelian gauge theory straightforwardly.

The Yang-Mills system is described by

$$L=-\tfrac{1}{4}F^a_{\mu\nu}F^a_{\mu\nu}\ . \tag{2.1}$$

The field equations are

$$F^a_{\mu\nu}=\partial_\mu A^a_\nu-\partial_\nu A^a_\mu+g\epsilon^{abc}A^b_\mu A^c_\nu\ , \tag{2.2}$$

$$\partial_\mu F^a_{\mu\nu}+g\epsilon^{abc}A^b_\mu F^c_{\mu\nu}=0\ . \tag{2.3}$$

We are interested in the class of solutions specified by

$$A^a_0=0\ ,\quad A^a_i=A^a_i(t)\ . \tag{2.4}$$

By the help of (2.4), Eq. (2.2) reduces to

$$F^a_{0i}=\partial_0 A^a_i\ , \tag{2.5}$$

$$F^a_{ij}=g\epsilon^{abc}A^b_i A^c_j\ . \tag{2.6}$$

Setting $\nu=0$ in (2.3), we obtain the Gauss law

$$g\epsilon^{abc}A^b_i F^c_{i0}=0 \tag{2.7}$$

or equivalently

$$A_i^b \partial_0 A_i^c - A_i^c \partial_0 A_i^b = 0 . \tag{2.8}$$

Setting $\nu = i$ in (2.3), we obtain the remaining field equations

$$\partial_0^2 A_i^a - g^2 \epsilon^{abc} \epsilon^{cde} A_j^b A_j^d A_i^e = 0 . \tag{2.9}$$

We can simplify the product of ϵ's to give

$$\partial_0^2 A_i^a + g^2 (A_i^a A_j^b - A_j^a A_i^b) A_j^b = 0 . \tag{2.10}$$

As pointed out by Baseyan *et al.*,[7] one can satisfy the Gauss law (2.8) by choosing

$$A_i^a = O_i^a f^a(t) \quad (a \text{ not summed}) , \tag{2.11}$$

where O_i^a are constant orthogonal matrices obeying

$$O_i^a O_i^b = \frac{1}{g^2} \delta^{ab} . \tag{2.12}$$

Then, Eq. (2.10) is satisfied if $f^a(t)$ obeys

$$\partial_0^2 f^a + \sum_{b \neq a} (f^b)^2 f^a = 0 . \tag{2.13}$$

Conversely, for any solution to (2.13), we can construct a vector potential A_i^a via (2.11) such that both the Yang-Mills field equations (2.2) and (2.3) and the gauge condition (2.4) are satisfied.

We can reproduce (2.13) from an effective Lagrangian

$$L = \tfrac{1}{2} \sum_a (\dot{f}^a)^2 - \tfrac{1}{4} \sum_a \sum_{b \neq a} (f^a)^2 (f^b)^2 . \tag{2.14}$$

This system has a positive-definite conserved energy

$$H = \tfrac{1}{2} \sum_a (\dot{f}^a)^2 + \tfrac{1}{4} \sum_a \sum_{b \neq a} (f^a)^2 (f^b)^2 . \tag{2.15}$$

In (2.14), (2.15), and hereafter, the overdots indicate time derivatives.

We can preserve the temporal gauge condition and the spatial independence of A_i^a in Eq. (2.4) by making an arbitrary global gauge transformation. In particular, we can choose the isospin directions to coincide with the x,y,z directions, giving

$$O_i^a = \frac{1}{g} \delta_i^a . \tag{2.16}$$

In this global gauge, we have

$$f^a = g A_a^a \quad (a \text{ not summed}) . \tag{2.17}$$

We shall consider some special cases.

(1) Assume $f^2 = f^3 = 0$, but $f^1 \neq 0$. We have a single equation

$$\ddot{f}^1 = 0 . \tag{2.18}$$

The solution to (2.18) is

$$f^1 = C_0 + C_1 t , \tag{2.19}$$

$$A_1^1 = (C_0 + C_1 t)/g . \tag{2.20}$$

This solution corresponds to a constant E field in the isospin and spatial 1-direction.

(2) Assume $f^3 = 0$, but $f^1, f^2 \neq 0$. We have a set of coupled equations

$$\ddot{f}^1 + (f^2)^2 f^1 = 0 , \tag{2.21}$$

$$\ddot{f}^2 + (f^1)^2 f^2 = 0 . \tag{2.22}$$

Nikolaevskii and Shur have studied these equations in Ref. 9. They showed that these equations are nonintegrable and admit no conserved integrals other than the trivial one given in (2.15). From this study, they draw an important conclusion that the classical Yang-Mills field theories are not integrable. In this paper, we shall study the detailed time dependence of these coupled equations.

In the global gauge (2.17), we find that the only nonvanishing A_μ^a are A_1^1 and A_2^2. These A's give rise to the following nonvanishing gauge fields:

$$E_1^1 \equiv F_{01}^1 = \dot{A}_1^1 ,$$

$$E_2^2 \equiv F_{01}^2 = \dot{A}_2^2 ,$$

and

$$B_3^3 \equiv F_{12}^3 = g A_1^1 A_2^2 .$$

In terms of E and B, the conserved quantity is

$$H = \frac{g^2}{2} [(E_1^1)^2 + (E_2^2)^2 + (B_3^3)^2] . \tag{2.23}$$

III. ADIABATIC APPROXIMATION

We now study (2.21) and (2.22). To simplify the notation, we introduce

$$u \equiv f_1^1 , \quad v \equiv f_2^2 , \tag{3.1}$$

and obtain

$$\ddot{u} + v^2 u = 0 , \tag{3.2}$$

$$\ddot{v} + u^2 v = 0 , \tag{3.3}$$

$$H = \tfrac{1}{2} (\dot{u}^2 + \dot{v}^2 + u^2 v^2) = \text{const.} \tag{3.4}$$

Note that we can scale $u \to \lambda u$, $v \to \lambda v$, $t \to t/\lambda$, and still keep (3.2) and (3.3) invariant. This scaling property implies that we can rescale H to $\frac{1}{2}$, giving

$$\dot{u}^2 + \dot{v}^2 + u^2 v^2 = 1 . \tag{3.5}$$

Equation (3.5) implies that all $u(t)v(t)$ are bounded by the hyperbolas $uv = \pm 1$. We may interpret (3.2) and (3.3) as the equations of motion for a "particle" of unit mass moving under the influence of a two-dimensional potential

$$V(u,v) = \tfrac{1}{2} u^2 v^2 . \tag{3.6}$$

The energy conservation alone does not rule out the possibility that the particle may eventually escape along the u or v axis. An escape solution corresponds to an asymptotic constant-E-field configuration along the 1- or 2-direction. As we shall see, such an escape will not occur no matter how long the system evolves.

Simple numerical study indicates that the solution is dominated either by large-u/small-v or by large-v/small-u periods. From time to time, the solution will flip over

from large-u periods to large-v periods and vice versa. In a large-u/small-v period, we have

$$|u| \gg 1, \quad v = O(1/u), \qquad \dot{u} = O(1), \quad \dot{v} = O(1). \tag{3.7}$$

Since $|\dot{u}| \ll |u|$ and $|\dot{v}| \gg |v|$, we can consider $u(t)$ as slowly varying and $v(t)$ as rapidly varying. Equation (3.3) describes the motion of a harmonic oscillator with a slowly varying frequency $u(t)$.

Using the adiabatic invariance theorem,[10] we have

$$v(t) = \frac{1}{[u_m u(t)]^{1/2}} \cos\left[\int^t u(t)dt + \phi\right], \tag{3.8}$$

where u_m and ϕ are integration constants describing the amplitude and the phase of $v(t)$. Next, we use the fact that v is rapidly varying, and replace v^2 in (3.2) by its time average, obtaining

$$\ddot{u} + \langle v^2 \rangle u = 0. \tag{3.9}$$

Since the average of $(\cos)^2$ is $\frac{1}{2}$, we have

$$\ddot{u} + \frac{1}{2u_m} = 0. \tag{3.10}$$

Thus, $u(t)$ described the free-fall motion of a particle under the influence of a constant acceleration, $-1/2u_m$. Substituting (3.8) into (3.5) and ignoring terms $O(1/u)$ or smaller, we have

$$\dot{u}^2 + u/u_m = 1. \tag{3.11}$$

Hence, we have $\dot{u} = 0$ at $u = u_m$. Equation (3.11) tells us that u_m is the maximum of u.

Physically, we can understand the bouncing of $u(t)$ as follows: As $u(t)$ moves to a larger and larger value, $v(t)$ oscillates faster and faster. In particular, the sum of its kinetic and potential energies, $\dot{v}^2 + u(t)^2 v^2$, increases linearly with $u(t)$. This increase of energy associated with v is compensated by a decrease of $\dot{u}^2$. At $u = u_m$, $\dot{u} = 0$ and the particle is forced to go back (see Fig. 1). This is very similar to the reflection of a charged particle in a magnetic bottle.[11]

The adiabatic approximation and Eq. (3.9) break down in the region $|u| \leq O(1)$. However, in this region, we have a nearly constant $\dot{u} \approx \pm 1$. As the particle moves through this region, we start a new free-fall motion with a different u_m' (see Fig. 1).

We now wish to relate u_m' to its preceding u_m. Since the adiabatic invariance breaks down in the middle region, we need to solve these equations under a different approximation. Fortunately, for a large u_m, we can find a region $-\epsilon |u_m| < u < \epsilon |u_m|$ with $0 < \epsilon \ll 1$ but $\epsilon |u_m| \gg 1$. In this region, we have $\dot{u}^2 = 1$ and $\ddot{u}$ being small. Then, we can rewrite (3.3) as

$$\frac{d^2 v}{du^2} + u^2 v = 0. \tag{3.12}$$

Since this equation is valid for $-\epsilon |u_m| < u < \epsilon |u_m|$ with $\epsilon |u_m| \gg 1$, it overlaps with the adiabatic solution (3.8) at both $u \to +\infty$ and $u \to -\infty$. This provides a link to u_m and u_m'.

The solutions to (3.12) are related to Bessel functions,

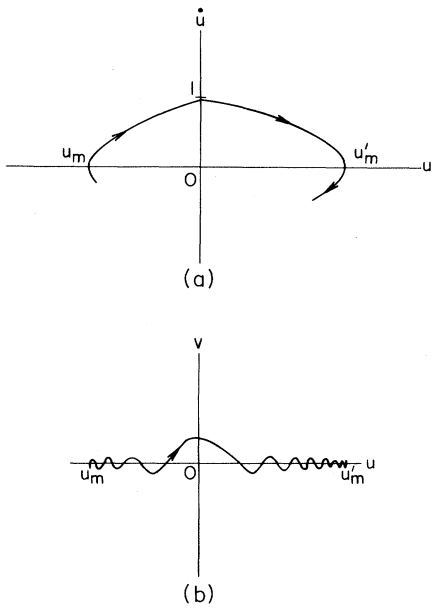

FIG. 1. A typical large-u solution with a crossing from negative to positive u. (a) The u-$\dot{u}$ plot is given approximately by two parabolas with vertices at u_m and u_m'. (b) In the u-v plot, the solution bounces back at both u_m and u_m'.

$$v = C_1 \sqrt{u}\, J_{1/4}(u^2/2) + C_2 \sqrt{u}\, J_{-1/4}(u^2/2). \tag{3.13}$$

We can study both the small-u and the large-u behavior of v. Using

$$J_\nu(z) = (\tfrac{1}{2}z)^\nu \sum \frac{(-\frac{1}{4}z^2)^k}{k!\Gamma(\nu + k + 1)} \tag{3.14}$$

we have the odd solution

$$\sqrt{u}\, J_{1/4}(u^2/2) = \frac{u}{\sqrt{2}} \sum \frac{(-1)^k (u/2)^{4k}}{k!\Gamma(k + 5/4)} \tag{3.15}$$

and the even solution

$$\sqrt{u}\, J_{-1/4}(u^2/2) = \sqrt{2} \sum \frac{(-1)^k (u/2)^{4k}}{k!\Gamma(k + 3/4)}. \tag{3.16}$$

We can obtain the large-u behavior of these odd and even solutions from the asymptotic formula of J_ν,

$$\sqrt{u}\, J_\nu(u^2/2) = \left[\frac{4}{\pi u}\right]^{1/2} \cos\left[\frac{u^2}{2} - \frac{\nu\pi}{2} - \frac{\pi}{4}\right] \qquad (|u| \to \infty, \arg u < \pi/2), \tag{3.17}$$

giving

$$\sqrt{u}\, J_{1/4}(u^2/2) = \left[\frac{4}{\pi u}\right]^{1/2} \cos\left[\frac{u^2}{2} - \frac{3\pi}{8}\right], \quad u \to \infty \tag{3.18a}$$

$$= -\left[\frac{4}{\pi |u|}\right]^{1/2} \cos\left[\frac{u^2}{2} - \frac{3\pi}{8}\right], \qquad u \to -\infty \tag{3.18b}$$

and

$$\sqrt{u}\,J_{-1/4}(u^2/2)=\left[\frac{4}{\pi u}\right]^{1/2}\cos\left[\frac{u^2}{2}-\frac{\pi}{8}\right],\quad u\to\infty \tag{3.19a}$$

$$=\left[\frac{4}{\pi\,|\,u\,|}\right]^{1/2}\cos\left[\frac{u^2}{2}-\frac{\pi}{8}\right],\quad u\to-\infty\ . \tag{3.19b}$$

Now, we are in the position to match the adiabatic solutions. We assume that a solution goes through $u=0$ from left ($u<0$) to right ($u>0$) (see Fig. 1). We assume further that this solution has the asymptotic forms

$$v=\frac{1}{\sqrt{u'_m u}}\cos\left[\int_{t_0}^{t}u(t)dt+\phi'\right]\ (u\to\infty) \tag{3.20a}$$

and

$$v=\frac{1}{\sqrt{u_m u}}\cos\left[\int_{t_0}^{t}u(t)dt+\phi\right](u\to-\infty)\ , \tag{3.20b}$$

where t_0 is chosen to be at the crossing $u(t_0)=0$. In the region $|\,u\,|\gg 1$ and $|\,u\,|<\epsilon\,|\,u_m\,|$ we have

$$v=\frac{1}{\sqrt{u'_m u}}\cos\left[\frac{u^2}{2}+\phi'\right]\ (u\to\infty) \tag{3.21a}$$

$$=\frac{1}{\sqrt{u_m u}}\cos\left[\frac{u^2}{2}+\phi\right](u\to-\infty)\ . \tag{3.21b}$$

In the following, when there is no danger of confusion, we shall denote $|\,u_m\,|$ by u_m and $|\,u'_m\,|$ by u'_m.

Comparing asymptotic formulas (3.18b), (3.19b), and (3.21b) at $u\to-\infty$, we have

$$-C_1\left[\frac{4}{\pi}\right]^{1/2}\cos\left[\frac{u^2}{2}-\frac{3\pi}{8}\right]+C_2\left[\frac{4}{\pi}\right]^{1/2}\cos\left[\frac{u^2}{2}-\frac{\pi}{8}\right]=\frac{1}{\sqrt{u_m}}\cos\left[\frac{u^2}{2}+\phi\right]\ . \tag{3.22}$$

Equation (3.22) implies

$$C_1\left[\frac{4}{\pi}\right]^{1/2}=\left[\frac{2}{u_m}\right]^{1/2}\cos\left[\phi-\frac{3\pi}{8}\right], \tag{3.23a}$$

$$C_2\left[\frac{4}{\pi}\right]^{1/2}=\left[\frac{2}{u_m}\right]^{1/2}\cos\left[\phi-\frac{\pi}{8}\right]\ . \tag{3.23b}$$

Next we examine asymptotic formulas (3.18a), (3.19a), and (3.21a) at $u\to\infty$, and obtain

$$C_1\left[\frac{4}{\pi}\right]^{1/2}\cos\left[\frac{u^2}{2}-\frac{3\pi}{8}\right]+C_2\left[\frac{4}{\pi}\right]^{1/2}\cos\left[\frac{u^2}{2}-\frac{\pi}{8}\right]=\frac{1}{\sqrt{u'_m}}\cos\left[\frac{u^2}{2}+\phi'\right]\ . \tag{3.24}$$

Substituting (3.23) into (3.24) and comparing the coefficients of $\cos(u^2/2)$ and $\sin(u^2/2)$, we have

$$\frac{1}{\sqrt{u'_m}}\cos\phi'=\frac{1}{\sqrt{u_m}}(\sqrt{2}\cos\phi+\sin\phi)\ , \tag{3.25a}$$

$$\frac{1}{\sqrt{u'_m}}\sin\phi'=-\frac{1}{\sqrt{u_m}}(\sqrt{2}\sin\phi+\cos\phi)\ . \tag{3.25b}$$

Hence, we have

$$\frac{u_m}{u'_m}=(\sqrt{2}\cos\phi+\sin\phi)^2+(\sqrt{2}\sin\phi+\cos\phi)^2=3+2\sqrt{2}\sin 2\phi \tag{3.26}$$

and

$$\tan\phi'=-\frac{\sqrt{2}\sin\phi+\cos\phi}{\sqrt{2}\cos\phi+\sin\phi}=-\frac{\sqrt{2}\tan\phi+1}{\sqrt{2}+\tan\phi}\ . \tag{3.27}$$

Equations (3.26) and (3.27) tell us how to obtain the new amplitude and phase from the old amplitude and phase. Note that both ϕ' and u'_m/u_m are functions of ϕ only, independent of u_m. In Fig. 2, we plot ϕ' and u'_m/u_m as functions of ϕ. The ratio u'_m/u_m is bounded between $3+2\sqrt{2}$ and $3-2\sqrt{2}$.

Outside the crossing region, $u(t)$ follows a free-fall trajectory in time. Thus we have reduced the large-u solutions to a set of algebraic iteration relations followed by free-fall motions. The identical treatment holds for large-v solutions as well.

IV. DISCRETE MAPS AND RANDOM-PHASE APPROXIMATION

A. Discrete maps

In the previous section, we have shown how to connect two large-u regions across a small-u region. Formulas (3.26) and (3.27) describe a mapping of (u_m,ϕ) to $(u'_m$ to

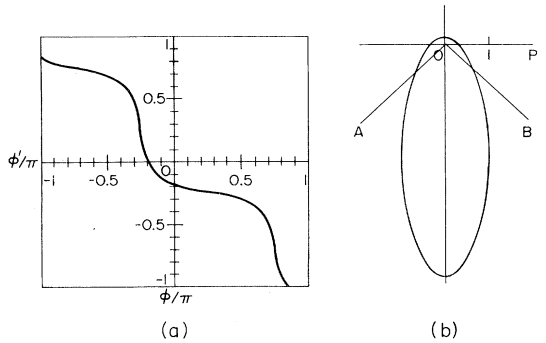

FIG. 2. (a) The phase ϕ' as a function of ϕ. (b) The ratio u_m/u'_m as a function of the phase angle ϕ. We use a polar coordinate representation where r is u_m/u'_m and the polar angle is 2ϕ. In this polar representation, the trajectory is an ellipse. Note that $u'_m=u_m$ (i.e., $r=1$) at $\phi=-3\pi/8$ (line $0A$) and at $\phi=-\pi/8$ (line $0B$).

ϕ') for a right-moving ($\dot{u}>0$) solution. For a left-moving solution ($\dot{u}<0$), Eqs. (3.21), (3.26), and (3.27) are modified with $\phi\rightarrow-\phi$.

As $u(t)$ passes through $u=0$ at $t=t_0$, reaches its maximum at u_m, and returns to $u=0$ again at $t=t_1$, we have to introduce two phases: A phase ϕ_0 associated with the crossing at t_0 and another phase ϕ_1 associated with the crossing at t_1. These two phases are related by

$$\phi_1=\phi_0+\int_{t_0}^{t_1} dt\, u(t) . \tag{4.1}$$

We can obtain $u(t)$ between t_0 and t_1 by a free-fall solution:

$$u(t)=(t-t_0)-\frac{1}{4u_m}(t-t_0)^2 \tag{4.2}$$

with

$$t_1-t_0=4u_m , \tag{4.3}$$

giving

$$\phi_1=\phi_0+\tfrac{8}{3}u_m{}^2 \quad (u_m>0) . \tag{4.4}$$

For a solution with negative u_m, we have

$$\phi_1=\phi_0-\tfrac{8}{3}u_m{}^2 \quad (u_m<0) . \tag{4.5}$$

In order to give a uniform treatment of right- and left-moving solutions, we introduce a new phase via

$$\begin{aligned}\theta&\equiv-\phi \quad \text{for } \dot{u}>0\\ &\equiv\phi \quad \text{for } \dot{u}<0 .\end{aligned} \tag{4.6}$$

Then we can describe the crossing of $u=0$ region and the free fall, for both the right- and left-moving solutions, by

$$u_m'=(3-2\sqrt{2}\sin2\theta)^{-1}u_m , \tag{4.7a}$$

$$\tan\theta'=-\frac{\sqrt{2}\tan\theta-1}{\sqrt{2}-\tan\theta} , \tag{4.7b}$$

$$u_m''=u_m' , \tag{4.8a}$$

$$\theta'+\theta''=\tfrac{8}{3}(u_m')^2 , \tag{4.8b}$$

respectively. Equations (4.7) and (4.8) describe the iterative mapping of the amplitude and phase of successive crossings.

It is straightforward to show that, in terms of $(1/u,\theta)$, the mapping defined by (4.7) and (4.8) are area preserving. In other words,

$$d\Gamma\equiv\frac{du_m}{u_m{}^2}d\theta \tag{4.9}$$

forms an invariant phase space under iteration.

B. Random-phase approximation

Iterative equations (4.7) and (4.8) are quite different from the well-known Chirikov map.[12] In the Chirikov map, we have a control parameter k. For small k, the mappings are restricted by the horizontal Kolmogrov-Arnol'd-Moser (KAM) curves.[13] At large k, the horizontal KAM curves disappear and the mappings can become very chaotic. In our iterative map (4.7) and (4.8), we do not have any control parameter. Our mappings appear to be intrinsically chaotic.

For a large u_m, $\theta''+\theta'=8u_m{}^2/3$ is large in comparison with 2π. Thus, a small variation in u_m will induce a large variation in θ''. To treat this large uncertainty statistically, we make a random-phase approximation by assuming θ'' to be completely random. Under this approximation, we can treat (4.7) as a one-dimensional random-walk problem in variable $\ln u_m$, giving

$$\ln u_m''=\ln u_m-\ln(3-2\sqrt{2}\sin2\theta) . \tag{4.10}$$

The variable θ in (4.10) is now considered as a random variable. The maximum and minimum of $(3-2\sqrt{2}\sin2\theta)$ are $3\pm2\sqrt{2}$. They lead to maximum forward and maximum backward steps in $\ln u$ of size 1.7627.

For a uniform θ distribution, Eq. (4.10) gives rise to a nonsymmetric random walk. Indeed, in terms of the step size variable

$$\lambda\equiv\ln u_m''/u_m=-\ln(3-2\sqrt{2}\sin2\theta) \tag{4.11}$$

we have

$$d\theta=\frac{e^{-\lambda}d\lambda}{2[8-(3-e^{-\lambda})^2]^{1/2}} . \tag{4.12}$$

Thus, a uniform distribution in θ implies a probability distribution $P(\lambda)d\lambda$ in λ with

$$\begin{aligned}P(\lambda)&=\frac{e^{-\lambda}}{\pi[8-(3-e^{-\lambda})^2]^{1/2}}\\ &=\frac{e^{-\lambda/2}}{\pi(6-2\cosh\lambda)^{1/2}} .\end{aligned} \tag{4.13}$$

We have inserted a factor $2/\pi$ in (4.13) for normalization. In Fig. 3, we have plotted $P(\lambda)$ as a function of λ. It is obvious that $P(\lambda)$ is in favor of backward walks. Indeed, the probability of a forward walk ($|u_m'|>|u_m|$) is only $\frac{1}{4}$, and the probability of a backward walk ($|u_m'|<|u_m|$) is $\frac{3}{4}$. The expectation value of λ is

$$\langle\lambda\rangle\equiv\langle\ln u_m'/u_m\rangle=-\ln2<0 . \tag{4.14}$$

This random-walk probability $P(\lambda)$ will support an equilibrium distribution $f(\xi)$ with $\xi\equiv\ln u_m$. We expect

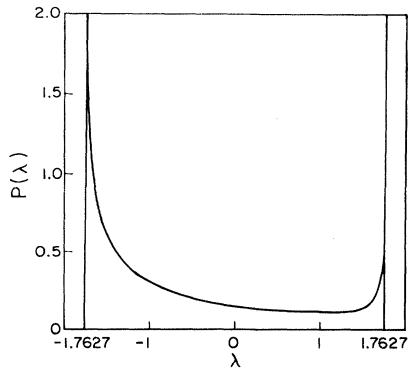

FIG. 3. Probability distribution function $P(\lambda)$ as a function of $\lambda=\ln(u_m''/u_m)$.

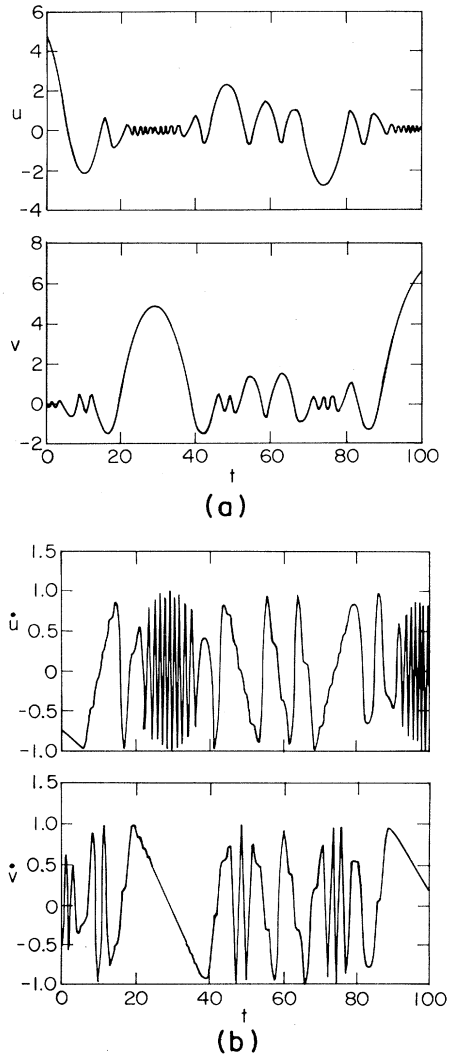

FIG. 4. The time evolution of a typical solution: (a) u and v as functions of t, (b) $\dot{u}$ and $\dot{v}$, which are the E fields, as functions of t.

that the distribution $f(\xi)$ becomes small at large ξ. The equilibrium condition implies that $f(\xi)$ should reproduce itself under iteration, giving

$$f(\xi)=\int d\xi' P(\xi-\xi')f(\xi') . \tag{4.15}$$

Substituting (4.13) into (4.15), we have

$$f(\xi)=\int \frac{d\xi'}{\pi}\frac{e^{-(\xi-\xi')/2}}{[6-2\cosh(\xi-\xi')]^{1/2}}f(\xi') , \tag{4.16}$$

where the ξ' integration is bounded by $|\xi-\xi'|\leq \ln(3+2\sqrt{2})=1.7627$. By inspection, we find the solution

$$f(\xi)=e^{-\xi} . \tag{4.17}$$

The other solution $f(\xi)=1$ is not physically acceptable.

For the equilibrium distribution (4.17), we can convert $f(\xi)d\xi$ to a distribution in u_m, giving

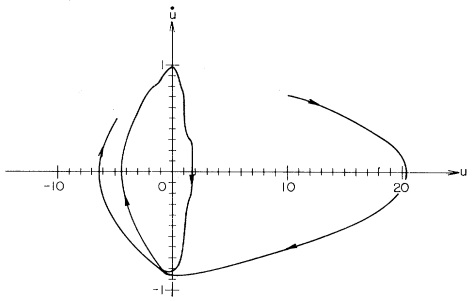

FIG. 5. A large-u trajectory in the u-$\dot{u}$ plot generated by numerical calculation. The trajectory consists of a sequence of parabolas.

$$f(\xi)d\xi=du_m/u_m^2 . \tag{4.18}$$

Distribution (4.18) agrees with the iterative invariant phase space $d\Gamma$ in (4.9) under the random-phase approximation. Note that the probability of having a large-u_m iteration becomes negligibly small as $u_m\to\infty$.

When we compute the distribution in u at a given instant, all u_m's with $u_m>u$ contribute. After including a $1/\dot{u}$ factor, we integrate (4.18) from 0 to ∞, giving a du/u distribution. This du/u distribution also agrees with the pure phase space $du\,d\dot{u}\,dv\,d\dot{v}$ by integrating out variables $(\dot{u},v,\dot{v})$ on the energy shell.

V. NUMERICAL CALCULATIONS AND PERIODIC SOLUTIONS

In Appendix A, we describe how to integrate the system numerically. We shall use the numerical method to illustrate our previous approximation as well as to construct periodic solutions.

A. Qualitative behavior

In Fig. 4, we illustrate the time evolution of a typical solution. Note that when u (or v) is large and slowly varying, v (or u) is small and rapidly varying. In a $u-\dot{u}$ plot, the large-u trajectory under the adiabatic approximation is a sequence of parabolas given by (3.11). Figure 5 is such a trajectory based on numerical calculation. As we can see,

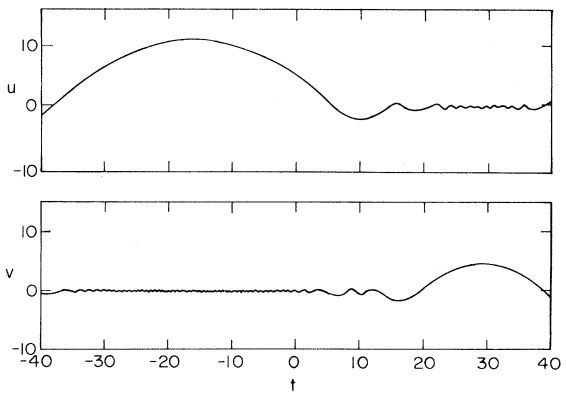

FIG. 6. A crossover from a large-u to a large-v behavior.

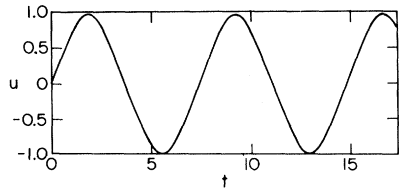

FIG. 7. The trivial periodic solution obtained by setting $u=v$. It corresponds to the cyclic return map ($u=0$, $\dot{v}>0$) generated by $v=0$ and $\dot{v}=1/\sqrt{2}$.

the adiabatic approximation becomes very good at $|u_m|>6$. Figure 6 represents a crossover from a large-u to a large-v behavior. In terms of field variables $E_1^1=\dot{u}$ and $E_2^2=\dot{v}$, such a crossover implies that the fast and slowly varying E fields are interchanged.

We can use the numerical method to verify our iterative maps. We find that our adiabatic formulas are exceedingly good for predicting u_m and ϕ. Even for u_m as small as 5, the discrepancies between the predicted and the actual values of u_m' and ϕ' are less than 1%. Hence, we can use the adiabatic formulas to study the long-time qualitative behavior of our system.

B. Periodic solutions

Periodic solutions play an important role in finite-temperature statistical mechanics and in the WKB treatment of field theories.[14] There is a trivial class of periodic solutions given by $u=\pm v$. Under these constraints, the problem becomes one dimensional. We are more interested in the genuine two-dimensional periodic solutions. We wish to emphasize that the periodic solutions that we construct correspond to non-self-dual periodic solutions of Yang-Mills fields. These non-self-dual solutions have not been fully studied before.

The simplest method to construct a periodic solution numerically is to use the technique of return map. We have four dynamical variables: $u,\dot{u},v,\dot{v}$. Energy conservation implies that only three of these are independent. If we specify v and $\dot{v}$ at the crossing plane $u=0$ with $\dot{u}>0$, all subsequent motion of u and v are determined. In particular, we can compute $(v,\dot{v})$ at the next crossing. This defines a return map. If $(v,\dot{v})$ at a future crossing agrees with the initial $(v,\dot{v})$, we have a periodic solution. Thus, we can obtain all periodic solutions by a two-parameter search in the return map.

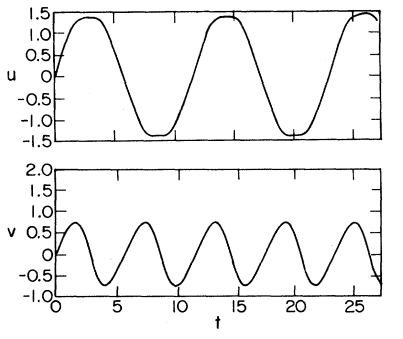

FIG. 8. A periodic solution with winding numbers 1/2. It corresponds to the cyclic return map generated by $u=v=0$ and $\dot{v}=0.5745$.

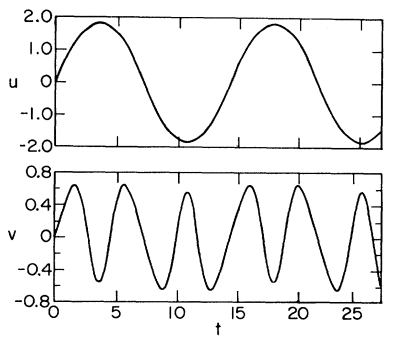

FIG. 9. A periodic solution with winding numbers 1/3, and generated by $u=v=0$ and $\dot{v}=0.5127$.

Because of the time-reversal symmetry of Eqs. (3.2) and (3.3), we can obtain two important classes of periodic solutions generated by the initial crossings at either $v=0$ or $\dot{v}=0$. These solutions are symmetric under time-reversal transformation about the initial crossing time t_0. If at one of the future returns t_1, we have once again $v=0$ or $\dot{v}=0$, then we have a similar time-reversal symmetry about t_1. Since two subsequent time-reversal symmetries imply a time-translational symmetry, we have automatically a periodic solution of period $T=2(t_1-t_0)$. These two classes of solutions are not mutually exclusive. Some of the solutions belong to both classes. Mixed crossing conditions (e.g., $v=0$ at t_0 and $\dot{v}=0$ at t_1) do not lead to any new solution.

We may classify these periodic solutions in the following manner: As a solution $(u(t),v(t))$ goes through a period T, the trajectories in the phase space $(u,\dot{u})$ and $(v,\dot{v})$ will circle around their origins p and q times, respectively. We denote this periodic solution by their winding numbers p/q.

In Figs. 7—16, we plot the first few periodic solutions. In Fig. 7, we have a trivial periodic solution with $u=v$. In Figs. 8—13, we have the periodic solutions associated with return maps with $v=0$. They are characterized by

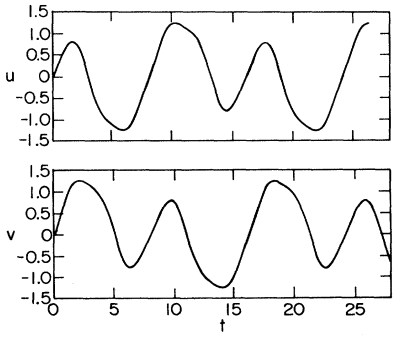

FIG. 10. A periodic solution with winding numbers 2/2, and generated by $u=v=0$ and $\dot{v}=0.7907$.

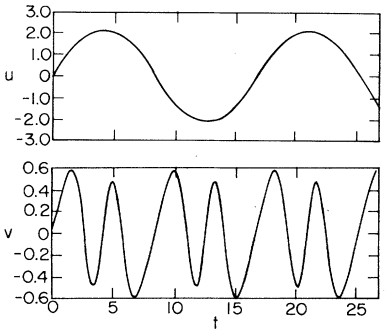

FIG. 11. A periodic solution with winding numbers 1/4, and generated by $u=v=0$ and $\dot{v}=0.4743$.

the winding numbers 1/2, 1/3, 2/2, 1/4, and 2/3. Note that the periodic solution 2/2 in Fig. 10 is different from the trial solution 1/1 in Fig. 7 which can also be interpreted as 2/2. The t dependence of u and v in Fig. 10 are interchanged after each half-period. Figures 12 and 13 describe two different periodic solutions with the identical winding numbers 2/3. The number of different periodic solutions increases rapidly as p and q increase. In Figs. 14—16, we plot the periodic solutions associated with return maps with $\dot{v}=0$. These maps have the winding numbers 1/2, 1/3, and 2/3. Figure 16 is identical to Fig. 12 with a shift of t_0. From each of these u's and v's, we generate a periodic non-self-dual solution to the original Yang-Mills equations.

We can obtain the large-p—small-q or large-q—small-p periodic solutions by finding the periodic cycles in iterative maps (4.7) and (4.8). The conditions $v=0$ and $\dot{v}=0$ correspond to the phase angles $\phi=-3\pi/8$ and $-\pi/8$, respectively.

VI. DISCUSSION

Even though the solutions that we have studied are very restrictive, we believe that the random character of the solutions is a general feature of the classical Yang-Mills system. Our finding supports the conclusion of Ref. 9 that the classical Yang-Mills fields are not exactly integrable. If the seemingly random flippings of gauge fields also occur at short distances, they may affect our understanding of QCD ground state and the quark-quark potential. At the moment, we do not know how important this effect is. A systematic study of the periodic solutions together with the WKB method[14] should provide us with some physical insights to this problem. It is important that we can generalize our method to include spatial dependence as well. In the following, we shall discuss in two simple cases what will happen if we include more degrees of freedom.

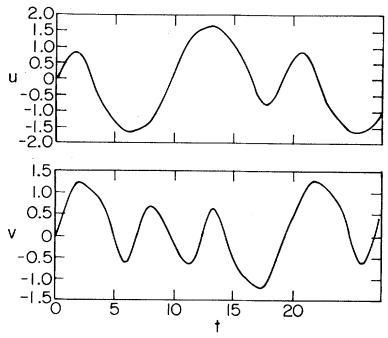

FIG. 13. This is a different periodic solution with the same winding numbers 2/3. It corresponds to the return map generated by $u=v=0$ and $\dot{v}=0.7808$.

A. Three coupled modes

We assume that A_i^a still has no $\vec{x}$ dependence as described in Sec. II. If none of the $f^{(a)}(a=1,2,3)$ in Eq. (2.13) is negligible, we encounter a coupled three-mode problem. For notational simplicity, we denote f^1, f^2, and f^3, by u, v, and w. When one of the variables, say u, is large and slowly varying, we have

$$\ddot{v}+u(t)^2v=0\,, \tag{6.1}$$

$$\ddot{w}+u(t)^2w=0\,, \tag{6.2}$$

and

$$\ddot{u}+(\langle v^2\rangle+\langle w^2\rangle)u=0\,. \tag{6.3}$$

Applying the adiabatic invariant method to (6.1) and (6.2), we have

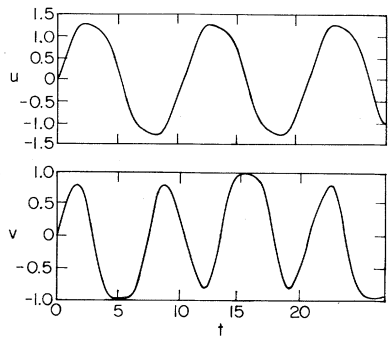

FIG. 12. A periodic solution with winding numbers 2/3 and generated by $u=v=0$ and $\dot{v}=0.6035$.

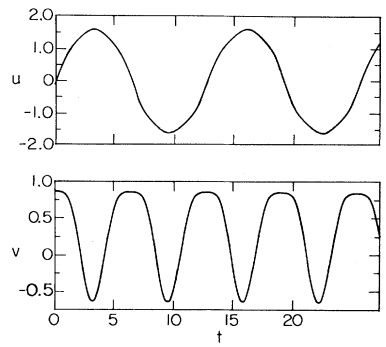

FIG. 14. A periodic solution with winding numbers 1/2, and generated by $u=0$, $v=0.8601$, and $\dot{v}=0$.

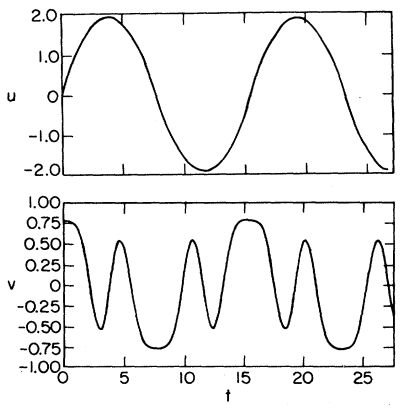

FIG. 15. A periodic solution with winding numbers 1/3 and generated by $u=0$, $v=0.7715$, and $\dot{v}=0$.

$$v(t)=\frac{1}{\sqrt{C_1 u}}\cos\left[\int u(t)dt+\phi_1\right], \tag{6.4}$$

$$w(t)=\frac{1}{\sqrt{C_2 u}}\cos\left[\int u(t)dt+\phi_2\right]. \tag{6.5}$$

The solution is now specified by two amplitudes (C_1,C_2) and two phases (ϕ_1,ϕ_2). The equation for u is still given by

$$\ddot{u}+1/(2u_m)=0 \tag{6.6}$$

with

$$\frac{1}{u_m}\equiv\frac{1}{C_1}+\frac{1}{C_2}. \tag{6.7}$$

When u goes from a large negative region to a large positive region, we obtain the mappings

$$(C_1,\phi_1)\rightarrow(C_1',\phi_1'), \tag{6.8a}$$

$$(C_2,\phi_2)\rightarrow(C_2',\phi_2'). \tag{6.8b}$$

Each of the mappings is given by (3.26) and (3.27). From C_1' and C_2', we obtain u_m' via (6.7).

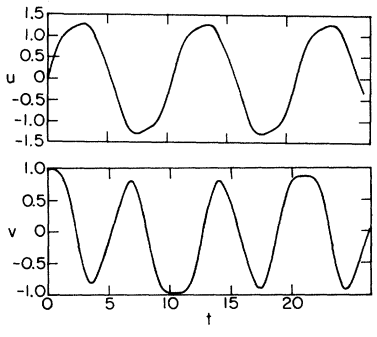

FIG. 16. A periodic solution with winding numbers 2/3 and generated by $u=0$, $v=0.9655$, and $\dot{v}=0$. This solution is the same as Fig. 12 with a shifting of origin and $u\rightarrow -u$.

The change of phases $\phi_1'\rightarrow\phi_1''$, $\phi_2'\rightarrow\phi_2''$ due to the free-fall motion of $u(t)$ is identical to that given in Eq. (4.8).

Thus, we have reduced the three-mode problem to a slightly more complicated mapping problem. A transition from a large-u solution to a large-v and/or large-w solution can only occur when u,v and/or w are of order 1. Hence, the three-mode problem is qualitatively identical to the two-mode problem discussed earlier.

B. Spatial dependence

We can introduce easily some spatial dependence into our solution. For instance we can consider solution of the form

$$A_0^a=A_3^a=0 \tag{6.9}$$

and $A_i^a(i=1,2)$ are functions of t and z only. The Gauss laws have the form

$$\epsilon^{abc}A_i^b\partial_0 A_i^c=0, \tag{6.10}$$

$$\epsilon^{abc}A_i^b\partial_3 A_i^c=0. \tag{6.11}$$

The equations of motion are

$$(\partial_0^2-\partial_3^2)A_i^a+g^2(A_i^aA_j^b-A_j^aA_i^b)A_j^b=0. \tag{6.12}$$

We can satisfy (6.10) and (6.11) automatically if we choose

$$A_i^a=O_i^a f^a(t,z)\ (a \text{ not summed}), \tag{6.13}$$

where O_i^a obeys

$$O_i^aO_i^b=\frac{1}{g^2}\delta_{ab}. \tag{6.14}$$

There are at most two independent O_i^a. Hence, we can only have two independent f's. For definiteness, we set $A_i^3=0$, giving

$$(\partial_0^2-\partial_3^2)\ddot{f}^1+(f^2)^2f^1=0, \tag{6.15}$$

$$(\partial_0^2-\partial_3^2)\ddot{f}^2+(f^1)^2f^2=0. \tag{6.16}$$

We now have a coupled $(1+1)$-dimensional field equation. Any solutions to (6.15) and (6.16) will give rise to a non-self-dual solution to the original Yang-Mills equations.

The systems (6.15) and (6.16) have a conserved energy and are also derivable from an effective Lagrange function.

ACKNOWLEDGMENTS

I wish to thank Barry Friedman for bringing Nikolaevskii and Shur's paper to my attention. I benefited from K. J. Shi for his work on a related problem. I thank the Research Board of the University of Illinois for providing me with some computer time. This work was supported in part by the National Science Foundation under Grant No. PHY-82-01948.

APPENDIX: NUMERICAL METHOD

We wish to approximate our equations

$$\ddot{u}+v^2u=0\,, \tag{A1}$$

$$\ddot{v}^2+u^2v=0 \tag{A2}$$

with a conserved energy

$$\dot{u}^2+\dot{v}^2+u^2v^2=1 \tag{A3}$$

by a set of difference equations. To avoid possible runaway solutions, we demand that the difference equations also support a positive-definite energy. One possible set of difference equations are

$$\frac{u_{n+1}+u_{n-1}-2u_n}{\delta^2}+v_n{}^2\frac{u_{n+1}+u_{n-1}}{2}=0\,, \tag{A4}$$

$$\frac{u_{n+1}+v_{n-1}-2v_n}{\delta^2}+u_n{}^2\frac{v_{n+1}+v_{n-1}}{2}=0\,, \tag{A5}$$

where δ is the time increment. Equations (A4) and (A5) give rise to a positive-definite conserved energy,

$$\text{energy}=\left[\frac{u_{n+1}-u_n}{\delta}\right]^2+\left[\frac{v_{n+1}-v_n}{\delta}\right]^2$$

$$+\tfrac{1}{2}(u_{n+1}{}^2v_n{}^2+v_{n+1}{}^2u_n{}^2)$$

$$=1\,. \tag{A6}$$

Equations (A4) and (A5) also preserve the time-reversal invariance. Given u_0,v_0,u_1,v_1 obeying (A6), we can use (A4) and (A5) to obtain u_n,v_n for all subsequent time. Even though the accuracy of $u(t),v(t)$ depends on the increment size δ, the qualitative behavior of $u(t)$ and $v(t)$ is quite insensitive to δ.

In our numerical calculation, we use typically $\delta=10^{-3}$. Occasionally, we use smaller δ's to test the stability of the solutions.

[1]G. K. Savvidy, Phys. Lett. 71B, 133 (1977); S. G. Matinyan and G. K. Savvidy, Nucl. Phys. B134, 539 (1978).

[2]N. K. Nielsen and P. Olesen, Nucl. Phys. B144, 376 (1978); Phys. Lett. 79B, 304 (1978).

[3]S. J. Chang and N. Weiss, Phys. Rev. D 20, 869 (1979); see also P. Sikivie, *ibid.* 20, 877 (1979).

[4]J. Ambjørn and P. Olesen, Nucl. Phys. B170, 60 (1980); B170, 265 (1980); see also S. J. Chang and G. J. Ni, Phys. Rev. D 26, 864 (1982).

[5]J. Mandula, Phys. Lett. 67B, 175 (1977).

[6]R. Jackiw and P. Rossi, Phys. Rev. D 21, 426 (1980).

[7]G. Z. Baseyan, S. G. Matinyan, and G. K. Savvidy, Pis'ma Zh. Eksp. Teor. Fiz. 29, 641 (1979) [JETP Lett. 29, 587 (1979)].

[8]For a brief review of the dynamo model, see, e.g., E. Bullard, in *Topics in Nonlinear Dynamics,* edited by S. Jorna (AIP, New York, 1978).

[9]E. S. Nikolaevskii and L. N. Shur, Pis'ma Zh. Eksp. Teor. Fiz. 36, 176 (1982) [JETP Lett. 36, 218 (1982)].

[10]See, e.g., L. D. Landau and E. M. Lifshitz, *Mechanics* (Pergamon, New York, 1969); H. Goldstein, *Classical Mechanics,* second ed. (Addison-Wesley, New York, 1980), pp. 531–540.

[11]See, e.g., F. Chen, *Introduction to Plasma Physics* (Plenum, New York, 1974).

[12]B. V. Chirikov, Phys. Rep. 52, 263 (1979).

[13]For discussions of the KAM theorem, see, e.g., M. V. Berry, in *Topics in Nonlinear Dynamics* (Ref. 8). A detailed proof was given in V. I. Arnol'd, Russ. Math. Surveys 18, 85 (1963).

[14]R. F. Dashen, B. Hasslacher, and A. Neveu, Phys. Rev. D 10, 4114 (1974); 10, 4130 (1974).